

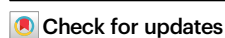
Synthesis, reactivity and nucleophilicity of carboranyl-B-Mg compound

Received: 19 May 2025

Yizhen Liu¹, Jie Zhang² & Zuowei Xie¹✉

Accepted: 4 September 2025

Published online: 08 October 2025



The reactivity of boron is most commonly defined by its Lewis acidity and its reactivity as an electrophile. Recently, nucleophilic boron anions have attracted tremendous research interest for offering alternative routes to a variety of boron compounds. Herein, we report the synthesis and structure of a nucleophilic boron anionic salt featuring an *exo*-polyhedral B-Mg bond. In sharp contrast to the known borylmetals, this bottleable compound does not have any heterocyclic backbones or supporting π -ligands. Its structure has been confirmed by single-crystal X-ray analyses. The calculated NPA charge of -0.503 at B(4) indicates the highly polarized B-Mg bond. It is shown to act as an unambiguous reactive nucleophile through its reactions with a broad range of organic, main-group, and transition-metal electrophiles.

Boron, occupying a pivotal position in the periodic table as carbon's electron-deficient neighbor, has long fascinated chemists with its unique electronic structure and versatile reactivity. As the fifth element with only three valence electrons, boron's natural electron deficiency has historically defined its chemical behavior, making tricoordinate boron compounds prototypical Lewis acids that dominate the landscape of boron chemistry. This electron poverty, while enabling remarkable electrophilic reactivity, has simultaneously rendered the development of nucleophilic boron species a formidable challenge^{1,2}.

The journey toward nucleophilic boron compounds began with the proposed intermediates in transition metal-catalyzed borylation reactions³. In these systems, the *d*-electrons of transition metals play a crucial stabilizing role through a delicate “push-pull” mechanism: the metal's filled *d*-orbitals donate electron density into boron's vacant *p*-orbital, while the metal's empty *d*-orbitals can accept electron density from boron. The landmark isolation of an *N*-heterocyclic boryl anion by Nozaki and Yamashita in 2006 marked a turning point in the field⁴. By employing two adjacent nitrogen atoms as stabilizing substituents, they achieved what had previously seemed impossible—a stable, isolable boryl anion (**I**, Fig. 1A). Such an anion finds wide applications in constructing diverse B-E bonds (E = B, C, P, Be, Mg, Cu, Sc, etc.)^{5,6}. This breakthrough opened floodgates of innovation, leading to various heteroatom-stabilized systems, including triazaborolyl anion (**II**, Fig. 1A)⁷ and Bpin-magnesium complex (**III**, Fig. 1A)⁸. These developments not only expanded the toolkit of synthetic chemistry but also

deepened our understanding of boron's electronic flexibility. However, they also revealed fundamental limitations: attempts to create analogous systems without heteroatom stabilization, such as CAAC-type boryl anions, consistently failed⁹, underscoring the essential role of heteroatoms in preventing boron's natural tendency toward electron deficiency. Apart from heteroatoms, neutral Lewis bases or anionic bases, were also applied to coordinate to the empty *p* orbital of the boron atom for stabilizing reactive boryl anions, as exemplified by boryls **IV–VIII** (Fig. 1A)^{10–15}.

Parallel to these advances in molecular boron chemistry, the field of cluster chemistry was making its own revolutionary progress with the development of carborane chemistry^{16–23}. Carboranes—polyhedral molecular clusters composed of boron and carbon atoms—represent a unique class of compounds that combine the electron-delocalized characteristics of aromatic systems with the three-dimensional geometry and exceptional stability of inorganic clusters¹⁶. Their robust structures, tunable electronic properties, and versatile reactivity profiles have found applications across an astonishing range of disciplines, from materials science²⁴ to medicine^{25,26}. What makes carboranes particularly intriguing for fundamental boron chemistry is their ability to stabilize unusual electronic configurations^{27–35}. The three-dimensional aromaticity of these clusters, combined with their electron-withdrawing character, creates electronic environments that are fundamentally different from those in conventional organic frameworks.

Recent work has demonstrated that carboranes can support both exceptionally strong Lewis acids and remarkably stable Lewis bases^{32,34}.

¹Shenzhen Grubbs Institute and Department of Chemistry, Southern University of Science and Technology, Shenzhen, Guangdong, China. ²Department of Chemistry, The Chinese University of Hong Kong, Shatin, China. ✉e-mail: xiezww@sustech.edu.cn

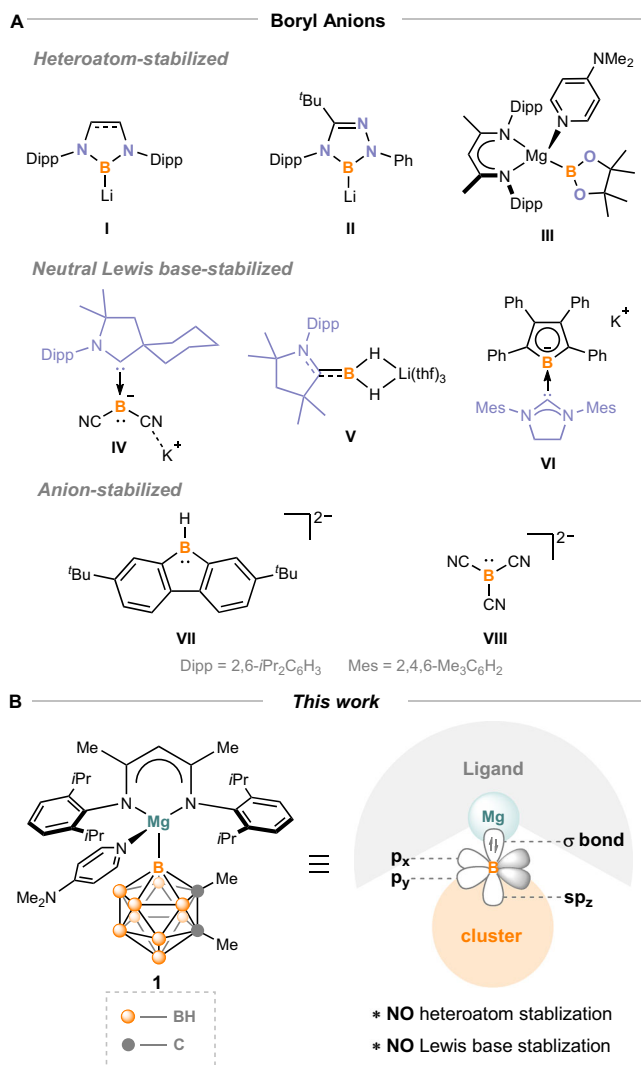


Fig. 1 | Boryl anions of classic boron and boron clusters. A Selected examples of boryl anions. **B** Structure of boron-centered carboranyl magnesium.

This dual nature suggested to us that carboranes might hold the key to solving one of boron chemistry's most persistent challenges: the creation of a nucleophilic boron center devoid of heteroatoms and π ligands. Our investigation was driven by a fundamental question: could the unique electronic and steric environment of a carborane cluster stabilize a nucleophilic boron center without relying on traditional heteroatom or Lewis base stabilization? Such an achievement would not only expand the boundaries of known boron chemistry but also provide new insights into the nature of chemical bonding in electron-delocalized systems. The implications would extend far beyond academic interest, potentially enabling new classes of reagents for synthetic chemistry, modular building blocks for materials science, and alternative reaction pathways in catalysis.

In this work, we report the realization of this long-sought goal: the synthesis, isolation, and comprehensive characterization of an unsupported nucleophilic boron-centered carboranyl magnesium compound (Fig. 1B). This species demonstrates that three-dimensional aromatic clusters can stabilize reactive centers in ways that differ from the reported examples. Through a combination of single-crystal X-ray crystallography, spectroscopic analysis, reactivity studies, and DFT calculations, we have established the unique electronic structure of this compound and its capacity to act as a nucleophilic boron reagent.

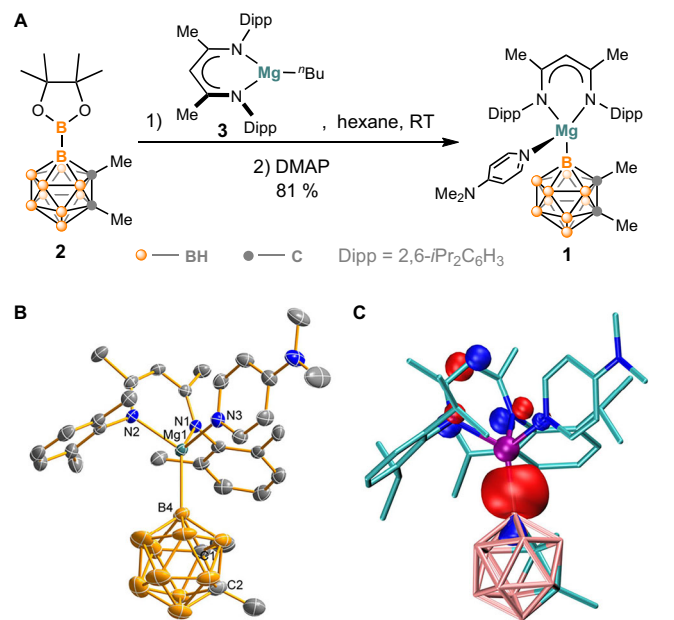


Fig. 2 | Synthesis and structure of B(4)-centered *o*-carboranyl magnesium 1.

A Synthetic route of **1**. **B** Single crystal X-ray structure of **1**. H atoms and the methyl groups of *i*Pr were omitted for clarity; thermal ellipsoids are set at the 50% probability level; selected bond distances (Å) and angles (°): Mg(1)–B(4) 2.325(3), Mg(1)–N(1) 2.100(2), Mg(1)–N(2) 2.090(2), Mg(1)–N(3) 2.160(2), N(2)–Mg(1)–N(1) 90.39(8), N(2)–Mg(1)–N(3) 100.28(9), N(1)–Mg(1)–N(3) 103.74(9), N(2)–Mg(1)–B(4) 122.54(11), N(1)–Mg(1)–B(4) 127.00(11), and N(3)–Mg(1)–B(4) 108.63(11). **C** HOMO of **1** calculated at B3LYP/6-311 + G (*d, p*) level of theory.

Results and discussion

Synthesis of B(4)-centered *o*-carboranyl magnesium (1)

We adopted the metathesis strategy to synthesize boron-centered carboranyl magnesium **1** as illustrated in Fig. 2A. Treatment of (BDI)MgⁿBu (**3**; BDI = HC(C(Me)N-2,6-*i*Pr₂C₆H₃)₂)^{8,36} with one equivalent of 1,2-dimethyl-4-Bpin-*o*-carborane (**2**) in *n*-hexane at room temperature gave, after adding one equivalent of 4-dimethylaminopyridine (DMAP), the boryl magnesium **1** in 81% isolated yield. The ¹¹B chemical shift of the B–Mg in **1** was observed at 1.9 ppm as a broad singlet, which was downfield shifted than that of magnesium boryl compound **III** (δ = –5.4 ppm)⁸, but was upfield shifted in comparison with those of reported *N*-heterocyclic boryl magnesium complexes (δ = 36.7–38.7 ppm)^{7,37,38}. Compound **1** was stable for several months in the solid state when stored in an Ar atmosphere at ambient temperature, but decomposed when its C₆D₆ solution was heated to 90 °C.

Structure of the boryl magnesium 1

In the single crystal structure of **1**, the icosahedral geometry of *o*-carborane moiety remains, featuring a B(4)–Mg bond (Fig. 2B). The bond length of B(4)–Mg is 2.325(3) Å, which is longer than the sum of covalent radii of B and Mg atoms (2.24 Å)³⁹, and lies within the range observed in the reported nitrogen^{7,37,38} or oxygen⁸ stabilized cyclic boryl magnesium species (2.28–2.37 Å). The Mg atom adopts a slightly distorted tetrahedral geometry, very similar to that observed in **III**. The distances between B(4) and adjacent B/C atoms of the carboranyl cage in **1** are slightly longer than those observed in 4-Bpin-*o*-carborane, respectively⁴⁰.

Density functional theory (DFT) calculations were carried out to understand the electronic properties of boryl magnesium **1**. The optimized structure fits well with the crystal structure of **1**. The highest occupied molecular orbital (HOMO) of **1** is predominantly localized on the σ bond between B(4) and Mg (Fig. 2C). This finding contrasts with those reported for *N/O*-heterocyclic boryl anions^{8,41}, where the HOMO

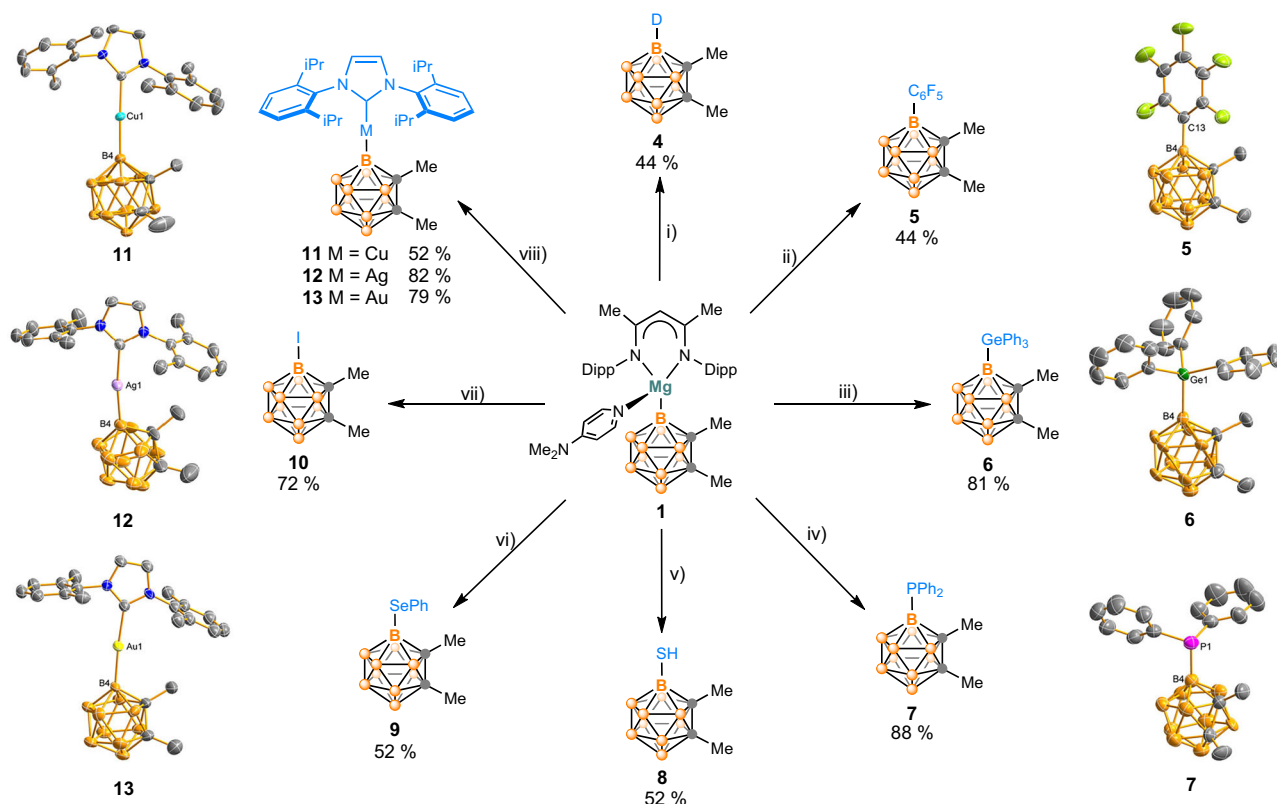


Fig. 3 | Reactions of **1 with various electrophiles and single crystal structures of some products.** (i) D₂O (3.0 equiv.), toluene, r.t., 1 h; (ii) C₆F₆ (1.5 equiv.), toluene, 70 °C, 24 h; (iii) Ph₃GeCl (1.0 equiv.), toluene, 60 °C, 24 h; (iv) Ph₂PCl (1.2 equiv.), toluene, r.t., 24 h; (v) S₈ (0.13 equiv.), toluene, 70 °C, 3 h; (vi) PhSeCl (1.0 equiv.),

toluene, r.t., 48 h; (vii) I₂ (1.4 equiv.), toluene, r.t., 1 h; (viii) IPrMCl (M = Cu, Ag, Au) (1.0 equiv.), toluene, r.t., 3 h for Cu, 24 h for Ag, 4 days for Au. Thermal ellipsoids are set at the 50% probability level, and the methyl groups of *i*Pr are omitted for clarity.

is partially delocalized across the *N/O*-heterocyclic ring, albeit with varying extents of delocalization. Additionally, the HOMO of **1** differs from those observed in boron cluster anions, such as B₆H₆²⁻, in which the HOMO lies across eight faces of the octahedron⁴². The localized nature of the HOMO of **1** suggests a propensity for charge aggregation. Natural population analysis (NPA) reveals that the B(4) atom in **1** carries a significant negative charge of −0.503, which is much more negative than those of the reported boryl anions, including the isolated boryl lithium **I** (+0.072)⁴ and Bpin magnesium **III** (+0.318)⁸. The value is even more negative than the most negative NPA charge of the lithioborane LiBH₂ (−0.37), which was previously reported by Schleyer using high-level ab initio calculations⁴³. The NPA charge of Mg(1) is +1.465, which is similar to that of **III** (+1.553)⁴⁴. The significant charge difference between B(4) and Mg results in a highly polarized B(4)–Mg bond, stabilizing **1**. The surrounding 2e–3c bonding interactions at B(4) and the bulky icosahedral geometry further enhance both the thermodynamic and kinetic stability of **1**¹⁶.

Nucleophilicity of **1**

The nucleophilicity of **1** was examined with various electrophiles (Fig. 3). Firstly, the reaction of **1** with D₂O was carried out, leading to the isolation of B(4)-deuterated *o*-carborane **4** in 44% yield. Then, electrophiles ranging from groups 14–17 were evaluated. Treatment of **1** with perfluorobenzene gave the corresponding pentafluorophenyl substituted *o*-carborane **5** in 44% isolated yield. Its structure was confirmed by single-crystal X-ray analyses. Such an S_NAr reaction with C₆F₆ is very similar to those observed for **I**⁴⁵ and **VIII**⁴⁶ shown in Fig. 1A. **1** reacted with Ph₃GeCl at room temperature, producing a carboranyl germanium **6** in 81% isolated yield. The structural characterization of **6** was validated through single-crystal X-ray analyses. Interaction of **1** with Ph₂PCl at room temperature afforded a carboranylphosphine **7** in

88% isolated yield. Its structure is shown in Fig. 3. Heating a mixture of **1** and S₈ in toluene at 70 °C generated 1,2-dimethyl-4-SH-*o*-carborane (**8**) in 52% yield. Reaction of **1** with PhSeCl gave the corresponding carboranyl selenium **9** in 52% isolated yield. Treatment of **1** with elemental iodine afforded a carboranyl iodide **10** in 72% isolated yield. Compound **1** was a very good transmetalation reagent for the synthesis of M–B bonded complexes. Reactions of **1** with IPrMCl (IPr = 1,3-bis(2,6-diisopropylphenyl)imidazol-2-ylidene, M = Cu, Ag, Au) produced the corresponding *o*-carboranyl Cu/Ag/Au complexes (**11–13**), which were fully characterized by multinuclear NMR and single crystal X-ray analyses. This result indicates that **1** may serve as a useful reagent for the construction of B–M (M = transition metals) bonded complexes. It is noteworthy that several transition metal complexes bearing a B–M bond were isolated as key intermediates from cage B–H metalation^{22,47–55}. The aforementioned nucleophilic reactions illustrated that **1** exhibited diverse reactivity behaviors comparable to those of carbanions, implying the potential application of this boryl magnesium of carborane as a powerful synthon for the functionalization of *o*-carborane.

In summary, we have developed a synthetic route to boron-centered carboranyl magnesium **1**, structurally characterized by single-crystal X-ray analysis. This compound features a highly polarized B–Mg bond, with the boron center (B(4)) bearing a notable NPA charge of −0.503. Unlike traditional boryl anions, which rely on heterocyclic frameworks or π -ligands for stabilization, this species derives its stability solely from the carboranyl cage. Demonstrating exceptional nucleophilicity, it reacts efficiently with diverse electrophiles, offering a versatile new tool for boryl compound synthesis. We expect this methodology to not only enable access to a wider range of boron-centered cluster anions but also to expand the utility of boron compounds in synthetic chemistry.

Methods

Procedure for the synthesis of compound 1

To a hexane solution of (BDI)MgⁿBu (**3**) prepared in situ, was added dropwise a hexane solution of compound **2** (298 mg, 1.0 mmol, 1.0 equiv.). After stirring the solution at room temperature for 1 h, *n*Bu₂Mg (0.6 mL, 0.6 mmol, 1.0 M in heptane, 0.6 equiv.) was added to the above solution in three portions within 7 h with stirring. The mixture was filtered, and the filter cake was washed with hexane (5 mL × 2). To the above solution was added 4-DMAP (122 mg, 1.0 mmol, 1.0 equiv.). The resulting mixture was stirred at room temperature for 1 h. The precipitate was filtered off, washed with hexane (5 mL × 2), and dried in a vacuum, generating **1** as a pale yellow powder (596 mg, 81%). Recrystallization from toluene/hexane (V/V=1:3) at −30 °C over a period of 10 days resulted in **1** as colorless crystals suitable for X-ray diffraction analysis.

Procedure for the synthesis of compound 4

To a toluene solution (10.0 mL) of **1** (499 mg, 0.68 mmol, 1.0 equiv.) was added dropwise D₂O (41 mg, 2.0 mmol, 3.0 equiv.). The resulting mixture was stirred at ambient temperature for 1 h, and then the mixture was filtered with silica gel. The filtrate was concentrated and purified by sublimation (100 °C, 1.5 mbar) to afford **4** as a white crystalline solid (52 mg, 44%).

Procedure for the synthesis of compound 5

To a toluene solution (3 mL) of **1** (200 mg, 0.27 mmol, 1.0 equiv.) was added dropwise C₆F₆ (76 mg, 0.41 mmol, 1.5 equiv.). The resulting mixture was stirred at 70 °C for 24 h. After removal of the solvent, the residue was purified by column chromatography on silica with hexane as eluent to give **5** as a white solid (40 mg, 44%). Recrystallization from CH₂Cl₂/hexane (V/V=1:5) at room temperature gave **5** as colorless crystals suitable for X-ray diffraction analysis.

Procedure for the synthesis of compound 6

Ph₃GcCl (46 mg, 0.14 mmol, 1.0 equiv.) was added to a toluene solution (2 mL) of **1** (100 mg, 0.14 mmol, 1.0 equiv.), and the resulting solution was stirred at 60 °C for 24 h. The mixture was filtered, and the filtrate was concentrated to dryness. The residue was purified by column chromatography on silica using hexane as eluent to give **6** as a white solid (54 mg, 81%). Slow evaporation of a CH₂Cl₂/hexane (V/V=1:3) solution at room temperature over a period of 5 days yielded **6** as colorless crystals suitable for X-ray diffraction analysis.

Procedure for the synthesis of compound 7

To a toluene solution (7 mL) of **1** (200 mg, 0.27 mmol, 1.0 equiv.) was added Ph₂PCl (73 mg, 0.33 mmol, 1.2 equiv.), and the resulting mixture was stirred at ambient temperature for 24 h. After addition of hexane (7 mL), the mixture was filtered and washed with a mixture of toluene and hexane (6 mL, *V*_{toluene}:*V*_{hexane} = 1:1). After removal of the solvent, the residue was purified by column chromatography on silica using hexane as eluent to afford **7** as a white solid (85 mg, 88%). Slow evaporation of a hexane solution of **7** produced colorless crystals suitable for X-ray diffraction analysis.

Procedure for the synthesis of compound 8

To a toluene solution (2 mL) of **1** (150 mg, 0.2 mmol, 1.0 equiv.) was added S₈ (6.5 mg, 0.2 mmol, 0.13 equiv.). After stirring at 70 °C for 3 h, the mixture was quenched with a dilute HCl solution (1.0 M, 5.0 mL). The organic layer was separated, and the aqueous solution was extracted with Et₂O (5 mL × 2). The organic portions were combined, dried over Na₂SO₄, and filtered. After removal of the solvent, the residue was sublimated (150 °C, 1.4 mbar) to give **8** as a white crystalline solid (21 mg, 52%).

Procedure for the synthesis of compound 9

PhSeCl (26 mg, 0.14 mmol, 1.0 equiv.) was added to a toluene solution (3 mL) of **1** (100 mg, 0.14 mmol, 1.0 equiv.), and the mixture was stirred at ambient temperature for 48 h. The resulting mixture was filtered. After removal of the solvent, the residue was purified by column chromatography on silica using hexane as eluent to afford **9** as a white solid (24 mg, 52%).

Procedure for the synthesis of compound 10

To a toluene solution (5 mL) of **1** (219 mg, 0.3 mmol, 1.0 equiv.) was added I₂ (107 mg, 0.42 mmol, 1.4 equiv.). The mixture was stirred at ambient temperature for 1 h. After removal of the solvent and addition of hexane (20 mL), the resulting solution was filtered and concentrated to dryness. The residue was purified by column chromatography on silica using hexane as eluent to provide **10** as a colorless oil (64 mg, 72%).

Procedure for the synthesis of compound 11

To a toluene solution (4 mL) of IPrCuCl (122 mg, 0.25 mmol, 1.0 equiv.) was added dropwise a toluene solution (4 mL) of **1** (185 mg, 0.25 mmol, 1.0 equiv.). The resulting mixture was stirred at ambient temperature for 3 h, followed by filtration. Slow evaporation of the solvent gave **11** as a light yellow crystalline solid (81 mg, 52%).

Procedure for the synthesis of compound 12

To a toluene solution (3 mL) of IPrAgCl (109 mg, 0.2 mmol, 1.0 equiv.) was added dropwise a toluene solution (5 mL) of **1** (150 mg, 0.2 mmol, 1.0 equiv.). After the mixture was stirred at ambient temperature for 24 h, the resulting solution was filtered. Slow evaporation of the solvent gave **12** as a light grey crystalline solid (110 mg, 82%).

Procedure for the synthesis of compound 13

To a toluene solution (1 mL) of IPrAuCl (62 mg, 0.1 mmol, 1.0 equiv.) was added dropwise a toluene solution (2 mL) of **1** (74 mg, 0.1 mmol, 1.0 equiv.). After the mixture was stirred at ambient temperature for 4 days, the resulting solution was filtered. Slow evaporation of the solvent gave **13** as a light grey crystalline solid (60 mg, 79%).

Data availability

All data generated in this study are provided in the Supplementary Information/Source Data file. Crystallographic data for the structures reported in this paper have been deposited at the Cambridge Crystallographic Data Centre, under deposition numbers CCDC 2433873 (**1**), 2433878 (**5**), 2433874 (**6**), 2433877 (**7**), 2433876 (**11**), 2433872 (**12**), and 2433875 (**13**). Copies of the data can be obtained free of charge via <https://www.ccdc.cam.ac.uk/structures/>. All data are available from the corresponding author upon request. Source data are provided with this paper.

References

- Gulyás, H. et al. Nucleophilic boron strikes back. *Pure Appl. Chem.* **84**, 2219–2231 (2012).
- Cid, J., Gulyás, H., Carbó, J. J. & Fernández, E. Trivalent boron nucleophile as a new tool in organic synthesis: reactivity and asymmetric induction. *Chem. Soc. Rev.* **41**, 3558–3570 (2012).
- Kays, D. L. & Aldridge, S. *Contemporary Metal Boron Chemistry I*, Vol. 130 (Springer, 2008).
- Segawa, Y., Yamashita, M. & Nozaki, K. Boryllithium: isolation, characterization, and reactivity as a boryl anion. *Science* **314**, 113–115 (2006).
- Yamashita, M. & Nozaki, K. in *Synthesis and Application of Organoboron Compounds* (eds. Fernández, E. & Whiting, A.) 1–37 (Springer, 2015).
- Duan, C. & Cui, C. Boryl-substituted low-valent heavy group 14 compounds. *Chem. Soc. Rev.* **53**, 361–379 (2024).

7. Lu, W., Hu, H., Li, Y., Ganguly, R. & Kinjo, R. Isolation of 1,2,4,3-triazaborol-3-yl-metal (Li, Mg, Al, Au, Zn, Sb, Bi) derivatives and reactivity toward CO and isonitriles. *J. Am. Chem. Soc.* **138**, 6650–6661 (2016).
8. Pécharman, A.-F. et al. Easy access to nucleophilic boron through diborane to magnesium boryl metathesis. *Nat. Commun.* **8**, 15022 (2017).
9. Kisu, H., Kosai, T., Iwamoto, T. & Yamashita, M. Synthesis and reduction of a cyclic (alkyl)(amino)bromoborane to generate a thermally labile cyclic (alkyl)(amino)boryl anion. *Chem. Lett.* **50**, 293–296 (2021).
10. Ruiz, D. A., Ung, G., Melaimi, M. & Bertrand, G. Deprotonation of a borohydride: synthesis of a carbene-stabilized boryl anion. *Angew. Chem. Int. Ed.* **52**, 7590–7592 (2013).
11. Arrowsmith, M. et al. Facile synthesis of a stable dihydroboryl $\{BH_2\}^-$ anion. *Angew. Chem., Int. Ed.* **57**, 15272–15275 (2018).
12. Braunschweig, H., Chiu, C.-W., Radacki, K. & Kupfer, T. Synthesis and structure of a carbene-stabilized π -boryl anion. *Angew. Chem. Int. Ed.* **49**, 2041–2044 (2010).
13. Gilmer, J. et al. The 9H-9-borafluorene dianion: a surrogate for elusive diarylboryl anion nucleophiles. *Angew. Chem. Int. Ed.* **59**, 5621–5625 (2020).
14. Landmann, J. et al. Deprotonation of a hydridoborate anion. *Angew. Chem. Int. Ed.* **56**, 2795–2799 (2017).
15. Budy, H., Gilmer, J., Trageser, T. & Wagner, M. Anionic organoboranes: delicate flowers worth caring for. *Eur. J. Inorg. Chem.* **2020**, 4148–4162 (2020).
16. Grimes, R. N. *Carboranes* 3rd edn (Elsevier, 2016).
17. Quan, Y., Tang, C. & Xie, Z. Nucleophilic substitution: a facile strategy for selective B–H functionalization of carboranes. *Dalton Trans.* **48**, 7494–7498 (2019).
18. Quan, Y., Qiu, Z. & Xie, Z. Transition-metal-catalyzed selective cage B–H functionalization of o-carboranes. *Chem. Eur. J.* **24**, 2795–2805 (2018).
19. Zhang, X. & Yan, H. Transition metal-induced B–H functionalization of o-carborane. *Coord. Chem. Rev.* **378**, 466–482 (2019).
20. Yu, W.-B., Cui, P.-F., Gao, W.-X. & Jin, G.-X. B–H activation of carboranes induced by late transition metals. *Coord. Chem. Rev.* **350**, 300–319 (2017).
21. Au, Y. K. & Xie, Z. Recent advances in transition metal-catalyzed selective B–H functionalization of o-carboranes. *Bull. Chem. Soc. Jpn.* **94**, 879–899 (2021).
22. Qiu, Z. & Xie, Z. A strategy for selective catalytic B–H functionalization of o-carboranes. *Acc. Chem. Res.* **54**, 4065–4079 (2021).
23. Zhang, J. & Xie, Z. A Strategy for regioselective B–H functionalization of o-carboranes via base metal catalysis. *Org. Chem. Front.* **10**, 3074–3079 (2023).
24. Nunez, R., Romero, I., Teixidor, F. & Vinas, C. Icosahedral boron clusters: a perfect tool for the enhancement of polymer features. *Chem. Soc. Rev.* **45**, 5147–5173 (2016).
25. Scholz, M. & Hey-Hawkins, E. Carbaboranes as pharmacophores: properties, synthesis, and application strategies. *Chem. Rev.* **111**, 7035–7062 (2011).
26. Issa, F., Kassiou, M. L. & Rendina, M. Boron in drug discovery: carboranes as unique pharmacophores in biologically active compounds. *Chem. Rev.* **111**, 5701–5722 (2011).
27. Wang, H., Zhang, J. & Xie, Z. Reversible photothermal isomerization of carborane-fused azaborole to borirane: synthesis and reactivity of carbene-stabilized carborane-fused borirane. *Angew. Chem. Int. Ed.* **56**, 9198–9201 (2017).
28. Wang, H., Wu, L., Lin, Z. & Xie, Z. Transition-metal-like behavior of monovalent boron compounds: reduction, migration, and complete cleavage of CO at a boron center. *Angew. Chem. Int. Ed.* **57**, 8708–8713 (2018).
29. Wang, H., Zhang, J., Lee, H. K. & Xie, Z. Borylene insertion into cage B–H bond: a route to electron-precise B–B single bond. *J. Am. Chem. Soc.* **140**, 3888–3891 (2018).
30. Wang, H., Zhang, J., Yang, J. & Xie, Z. Synthesis, structure, and reactivity of acid-free neutral oxoborane. *Angew. Chem. Int. Ed.* **60**, 19008–19012 (2021).
31. Liu, Y., Su, B., Dong, W., Li, Z. H. & Wang, H. Structural characterization of a boron(III) η^2 - σ -silane-complex. *J. Am. Chem. Soc.* **141**, 8358–8363 (2019).
32. Liu, Y., Dong, W., Li, Z. H. & Wang, H. Methane activation by a boronium complex. *Chem* **7**, 1843–1851 (2021).
33. Yao, S. et al. Changing the reactivity of zero- and mono-valent germanium with a redox non-innocent bis(silylenyl)carborane ligand. *Angew. Chem. Int. Ed.* **60**, 14864–14868 (2021).
34. Xiong, Y., Dong, S., Yao, S., Zhu, J. & Driess, M. Unexpected white phosphorus (P4) activation modes with silylene-substituted o-carboranes and access to an isolable 1,3-diphospha-2,4-disilabutadiene. *Angew. Chem. Int. Ed.* **61**, e202205358 (2022).
35. Zhang, C., Wang, J., Su, W., Lin, Z. & Ye, Q. Synthesis, characterization, and density functional theory studies of three-dimensional inorganic analogues of 9,10-diboraanthracene—a new class of Lewis superacids. *J. Am. Chem. Soc.* **143**, 8552–8558 (2021).
36. Dove, A. P. et al. Low coordinate magnesium chemistry supported by a bulky β -diketiminato ligand. *Dalton Trans.* **15**, 3088–3097 (2003).
37. Yamashita, M., Suzuki, Y., Segawa, Y. & Nozaki, K. Synthesis, structure of borylmagnesium, and its reaction with benzaldehyde to form benzoylborane. *J. Am. Chem. Soc.* **129**, 9570–9571 (2007).
38. Dange, D., Paparo, A. & Jones, C. Synthesis and characterization of a magnesium boryl and a beryllium-substituted diazaborole. *Chem. Asian J.* **15**, 2447–2450 (2020).
39. Cordero, B. et al. Covalent radii revisited. *Dalton Trans.* **2008**, 2832–2838 (2008).
40. Cheng, R., Qiu, Z. & Xie, Z. Iridium-catalysed regioselective borylation of carboranes via direct B–H activation. *Nat. Commun.* **8**, 14827 (2017).
41. Yamashita, M., Suzuki, Y., Segawa, Y. & Nozaki, K. Crystal structure of boryllithium with two THF molecules and DFT analysis of its property as a boryl anion. *Chem. Lett.* **37**, 802–803 (2008).
42. Mu, X. et al. Sterically unprotected nucleophilic boron cluster reagents. *Chem* **5**, 2461–2469 (2019).
43. Wagner, M., Hommes, N., Noth, H. & Schleyer, P. V. Lithioboranes. A theoretical study. *Inorg. Chem.* **34**, 607–614 (1995).
44. McMullin, C. L., Neale, S. E. & Young, G. L. A computational study into the mechanism of B–B bond cleavage in a magnesium(II) diborate complex. *Eur. J. Inorg. Chem.* **27**, e202300393 (2024).
45. Segawa, Y., Suzuki, Y., Yamashita, M. & Nozaki, K. Chemistry of boryllithium: synthesis, structure, and reactivity. *J. Am. Chem. Soc.* **130**, 16069–16079 (2008).
46. Landmann, J., Hennig, P. T., Ignat'ev, N. V. & Finze, M. Borylation of fluorinated arenes using the boron-centred nucleophile $B(CN)_3^{2-}$ —a unique entry to aryltricyanoborates. *Chem. Sci.* **8**, 5962–5968 (2017).
47. Lin, F. et al. Palladium-catalyzed selective five-fold cascade arylation of the 12-vertex monocarborane anion by B–H activation. *J. Am. Chem. Soc.* **140**, 13798–13807 (2018).
48. Shen, Y. et al. Synthesis and full characterization of an iridium B–H activation intermediate of the monocarba-closo-dodecaborate anion. *Chem. Commun.* **53**, 176–179 (2017).
49. Wang, Y.-P., Zhang, L., Lin, Y.-J., Li, Z.-H. & Jin, G.-X. Selective B(4)–H activation of an o-carboranylthioamide based on a palladium precursor. *Chem. Eur. J.* **23**, 1814–1819 (2017).
50. Shen, Y., Liu, J., Sattasathuchana, T., Baldrige, K. K. & Duttwyler, M. Transition metal complexes of a monocarba-closo-dodecaborate

- ligand via B–H activation. *Eur. J. Inorg. Chem.* **2017**, 4420–4424 (2017).
51. Cui, P.-F., Gao, Y., Guo, S.-T. & Jin, G.-X. Regioselective B–H/C–H bond activation at Azo-substituted carboranes induced by half-sandwich iridium(III) complex. *Chin. J. Chem.* **39**, 281–287 (2021).
52. Guo, S.-T., Cui, P.-F., Yuan, R.-Z. & Jin, G.-X. Transition metal-mediated B(4)–H hydroxylation/halogenation of o-carboranes bearing a 2-pyridylsulfenyl ligand. *Chem. Commun.* **57**, 2412–2415 (2021).
53. Quan, Y. & Xie, Z. Iridium catalyzed regioselective cage boron alkenylation of o-carboranes via direct cage B–H activation. *J. Am. Chem. Soc.* **136**, 15513–15516 (2014).
54. Lyu, H., Zhang, J., Yang, J., Quan, Y. & Xie, Z. Catalytic regioselective cage B(8)–H arylation of o-carboranes via “Cage-Walking” strategy. *J. Am. Chem. Soc.* **141**, 4219–4224 (2019).
55. Cao, H.-J. et al. Variable metal chelation modes and activation sequence in Pd-catalyzed B–H poly-arylation of carboranes. *ACS Catal.* **11**, 14047–14057 (2021).

Acknowledgements

We gratefully acknowledge the financial support from the National Natural Science Foundation of China (project no. 22331005 to Z.X. and 22301120 to Y.L.) and the Shenzhen Science and Technology Program (project no. KQTD20221101093558015 to Z.X. and RCBS20231211090650090 to Y.L.). J.Z. thanks the Research Grants Council of HKSAR (Project no. 14301223 to J.Z.).

Author contributions

Z.X. generated and managed the project. Y.L. carried out the experiments and structural determination of the reaction products and prepared the supplementary information. J.Z. carried out the DFT calculations. Y.L. and Z.X. prepared the manuscript.

Competing interests

The authors declare no competing interests.

Additional information

Supplementary information The online version contains supplementary material available at <https://doi.org/10.1038/s41467-025-64017-6>.

Correspondence and requests for materials should be addressed to Zuowei Xie.

Peer review information *Nature Communications* thanks Chunming Cui, Marc-Etienne Moret, and the other anonymous reviewer(s) for their contribution to the peer review of this work. A peer review file is available.

Reprints and permissions information is available at <http://www.nature.com/reprints>

Publisher's note Springer Nature remains neutral with regard to jurisdictional claims in published maps and institutional affiliations.

Open Access This article is licensed under a Creative Commons Attribution-NonCommercial-NoDerivatives 4.0 International License, which permits any non-commercial use, sharing, distribution and reproduction in any medium or format, as long as you give appropriate credit to the original author(s) and the source, provide a link to the Creative Commons licence, and indicate if you modified the licensed material. You do not have permission under this licence to share adapted material derived from this article or parts of it. The images or other third party material in this article are included in the article's Creative Commons licence, unless indicated otherwise in a credit line to the material. If material is not included in the article's Creative Commons licence and your intended use is not permitted by statutory regulation or exceeds the permitted use, you will need to obtain permission directly from the copyright holder. To view a copy of this licence, visit <http://creativecommons.org/licenses/by-nc-nd/4.0/>.

© The Author(s) 2025